Revue des Energies Renouvelables Vol. 15 N°1 (2012) 155 – 164
DOI: https://doi.org/10.54966/jreen.v15i1.308

Numerical study of external turbulent flow

Mohamed Mammar [1*] and Azeddine Soudani [2†]

[1] Thermal and Geothermal Division
Development Center of Renewable Energies, CDER
B.P. 62, Route de l'Observatoire, Algiers, Algeria
[2] Energetics Applied Physics Laboratory, Department of Physics
Faculty of Science, Hadj Lakhdar University
1, Av. Chahid Boukhlouf Mohamed El Hadi, Batna, Algeria

(reçu le 25 Février 2012 – accepté le 30 Mars 2012)

Abstract - *Flow around a cylinder on a fixed-bed open- channel is numerically studied. A CFD code is executed to analyze the flow fields and the kinetic energy field around the cylinder. A system of equations of two-dimensional and horizontal flow is obtained by the integration of the continuity and momentum equation for turbulent flow using (k - ε) standard model. The turbulent stresses are then expressed with the eddy-viscosity concept. The numerical simulation was done for four flows cases with different velocities. From the numerical results, the expected alteration of the flow field due to the presence of the cylinder is evident, notably the wake behind the cylinder. The measured velocities in the longitudinal and transversal directions and the kinetic energy are compared with those of the numerical simulation.*

Résumé - *Nous présentons ici l'étude de l'écoulement à surface libre autour d'un cylindre dans un canal à fond fixe. L'étude numérique a nécessité l'exécution d'un code CFD qui permet d'analyser le champ des vitesses et le champ de l'énergie cinétique autour du cylindre. L'intégration des équations de continuité et de quantité du mouvement pour l'écoulement turbulent a permis d'obtenir un système d'équations pour un écoulement bidimensionnel horizontal. Par l'intégration des équations de quantité de mouvement, on obtient un terme de diffusion-dispersion qui contient les tensions de turbulence et de dispersion. Les tensions de turbulence sont exprimées par le concept de viscosité turbulente. Quatre cas d'écoulement selon différents paramètres hydraulique ont été simulés numériquement. Les résultats démontrent clairement l'influence du cylindre sur la structure de l'écoulement, notamment dans la zone du sillage en aval du cylindre. Les vitesses mesurées dans les directions longitudinale et transversale confirment les résultats numériques, notamment des vecteurs de vitesse en amont du cylindre et le long de son périmètre. L'énergie cinétique turbulente obtenue par la simulation numérique a pu être comparée avec les mesures. Le modèle (k - ε) a sous-estimé les valeurs mesurées. Il paraît que ce problème provient de la difficulté du calcul de la génération d'énergie cinétique turbulente prés du bord solide. Ce problème a été identifié et discuté en détail.*

Keywords: Turbulence - Obstacle - Exterior flow - CFD – Stress.

1. INTRODUCTION

This work is a part of the numerical study of exterior turbulent flow around an obstacle. This class of flow has, in fact, complex physical phenomena that are difficult to be calculated. The large separations, the three-dimensional nature of these flows, the

* mohamed.mammar@cder.dz
† soudani.azeddine@yahoo.fr

presence of organized structures in turbulent flow and their nonlinear interactions with other scales, all of them need to reconsider the existing models in order to perform simulations.

This type of flow occurs in a variety of situations, such as flow around bridge piers, and around different types of junctions. For the flow around a bridge pier in a fixed-bed channel, the existence of vortices from the cylinder creates a scour hole. This local scour may lead to the destruction of the bridge pier.

The objective of this study is to gain a better understanding of the dynamic flow field and its structure of turbulence around a cylinder.

2. DEFINITION OF THE PROBLEM

Our study concerns the area that contains the cylinder. The geometry of the system is presented in the Figure 1:

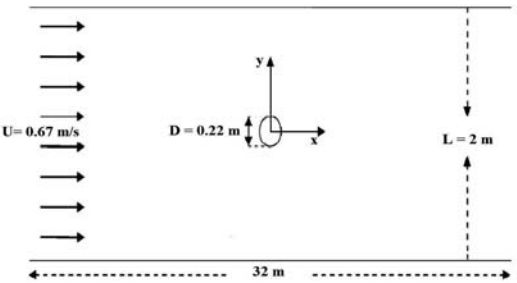

Fig. 1: Configuration of the flow around a cylinder, [1]

3. APPLICATION OF STANDARD ($k-\varepsilon$) MODEL

3.1 Assumptions

- The flow is assumed to be two-dimensional in which:

$$w = 0$$

$$\frac{\partial w u}{\partial z} = \frac{\partial w v}{\partial z} = \frac{\partial w w}{\partial z} = 0$$

$$\frac{\partial}{\partial z}\left(\nu_t \frac{\partial u}{\partial z} \right) = \frac{\partial}{\partial z}\left(\nu_t \frac{\partial v}{\partial z} \right) = \frac{\partial}{\partial z}\left(\nu_t \frac{\partial w}{\partial z} \right) = 0$$

$$\frac{\partial w}{\partial t} = \frac{\partial u w}{\partial x} = \frac{\partial v w}{\partial y} = \frac{\partial}{\partial x}\left(\nu_t \frac{\partial w}{\partial x} \right)$$
$$= \frac{\partial}{\partial y}\left(\nu_t \frac{\partial w}{\partial y} \right) = \frac{1}{\rho} \times \frac{\partial p}{\partial z} = \frac{\partial}{\partial x}\left(\nu_t \frac{\partial u}{\partial z} \right) = \frac{\partial}{\partial y}\left(\nu_t \frac{\partial v}{\partial z} \right) = 0$$

$$g_x = g_y = g_z = 0$$

$$\tau_{zz} = \tau_{xz} = \tau_{yz} = 0$$

$$\frac{\partial w k}{\partial z} = \frac{\partial w \varepsilon}{\partial z} = 0$$

$$\frac{\partial}{\partial z}\left(\frac{\nu_t}{\sigma_k} \times \frac{\partial k}{\partial z} \right) = \frac{\partial}{\partial z}\left(\frac{\nu_t}{\sigma_\varepsilon} \times \frac{\partial \varepsilon}{\partial z} \right) = 0$$

- The density of the fluid (water) is constant, $\rho = 999.2\ \mathrm{kg/m^3}$.
- The kinematic viscosity of the fluid is constant, $\nu = 9.959 \times 10^{-7}\ \mathrm{m^2/s}$.
- The flow is uniform at the entrance $U(0, y) = 0.67\,\mathrm{m/s}$. Then, the governing equations of the system become:

$$\frac{\partial u}{\partial t} + \frac{\partial uu}{\partial x} + \frac{\partial vu}{\partial y} - \frac{\partial}{\partial x}\left(\nu_t \frac{\partial u}{\partial x} \right) - \frac{\partial}{\partial y}\left(\nu_t \frac{\partial u}{\partial y} \right) = -\frac{1}{\rho} \times \frac{\partial p}{\partial x} + \frac{\partial}{\partial x}\left(\nu_t \frac{\partial u}{\partial x} \right) + \frac{\partial}{\partial y}\left(\nu_t \frac{\partial v}{\partial x} \right)$$

$$\frac{\partial v}{\partial t} + \frac{\partial uv}{\partial x} + \frac{\partial vv}{\partial y} - \frac{\partial}{\partial x}\left(\nu_t \frac{\partial}{\partial x} \right) - \frac{\partial}{\partial y}\left(\nu_t \frac{\partial v}{\partial y} \right) = -\frac{1}{\rho} \times \frac{\partial p}{\partial y} + \frac{\partial}{\partial x}\left(\nu_t \frac{\partial u}{\partial y} \right) + \frac{\partial}{\partial y}\left(\nu_t \frac{\partial v}{\partial y} \right)$$

$$\frac{\partial k}{\partial t} + \frac{\partial uk}{\partial x} + \frac{\partial vk}{\partial y} - \frac{\partial}{\partial x}\left(\frac{\nu_t}{\sigma_k} \times \frac{\partial k}{\partial x} \right) - \frac{\partial}{\partial y}\left(\frac{\nu_t}{\sigma_k} \times \frac{\partial u}{\partial y} \right) = G - \varepsilon$$

$$\frac{\partial \varepsilon}{\partial t} + \frac{\partial u\varepsilon}{\partial x} + \frac{\partial v\varepsilon}{\partial y} - \frac{\partial}{\partial x}\left(\frac{\nu_t}{\sigma_\varepsilon} \times \frac{\partial \varepsilon}{\partial x} \right) - \frac{\partial}{\partial y}\left(\frac{\nu_t}{\sigma_\varepsilon} \times \frac{\partial \varepsilon}{\partial y} \right) = \frac{\varepsilon}{k} \times (c_1 \times G - c_2 \times \varepsilon)$$

where,

$$G = \nu_t \times \left\{ 2\left(\frac{\partial u}{\partial x} \right)^2 + \left(\frac{\partial u}{\partial y} + \frac{\partial v}{\partial x} \right)\frac{\partial u}{\partial y} + \left(\frac{\partial v}{\partial x} + \frac{\partial u}{\partial y} \right)\frac{\partial v}{\partial x} + 2 \times \left(\frac{\partial v}{\partial y} \right)^2 \right\}$$

3.2 Initial and boundary conditions

- As we indicated earlier in this paper, the boundary conditions and initial condition are based on the experimental work of Yulistiyanto, [1].

So the initial and boundary conditions are:

$$U(-16, (-1 \le y \le 1), t \ge 0) = 0.67$$

$$V(-16, (-1 \le y \le 1), t \ge 0) = 0$$

- The walls of the channel

$$V(-16 \le x \le 16, -1, t \ge 0) = 0$$

$$v\,(-16 \le x \le 16,\ 1,\ t \ge 0) \;=\; 0$$

- Cylinder

$$u\,(x,\ y,\ t \ge 0) \;=\; v\,(x,\ y,\ t \ge 0) \;=\; 0$$

where,

$$\sqrt{x^2 + y^2} \;=\; 0.11\ \text{m}$$

- Outlet pressure

$$p\,(16,\ -1 \le y \le 1,\ t \ge 0) \;=\; p_{atm}$$

For high Reynolds number flows, the viscous efforts are much smaller compared to those of turbulence and can be neglected. These efforts are proportional to the gradient of velocity by using the concept of Boussinesq viscosity.

3.3 Meshing

- We choose triangular control volume, and the discretization method is as following in the figure 2.

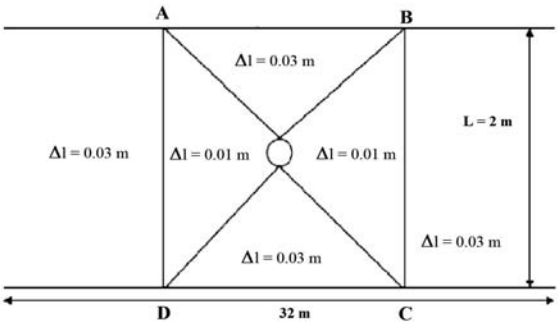

Fig. 2: System meshing method

A very concentrated mesh is used around the cylinder (in downstream and upstream) with a step of $\Delta l = 0.01$. Somewhere else, a triangular mesh is used with a step of $\Delta l = 0.03$. So, we get 249.395 nodes.

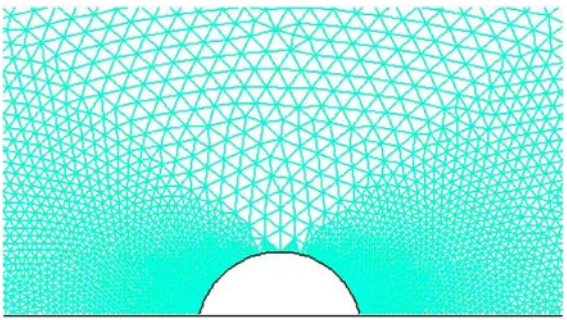

Fig. 3: Display of grid

4. RESULTS

4.1 Fields with Re=148000

a- Averaged speeds: we present in the Figure 4 the stream lines of the mean flow at $Re = 148\,000$ at the downstream of the cylinder.

The flow is symmetrical with respect to the axis $y = 0$ and conventionally attached to the two vortices cylinder mainly resulting from the averaging of alternating Von Karman vortices.

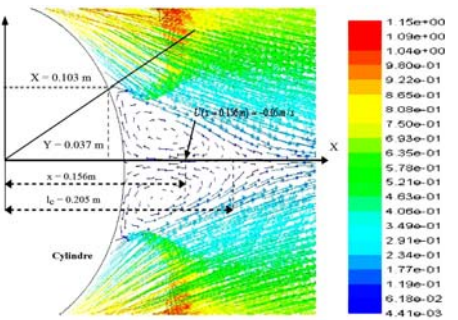

Fig. 4: Streamlines $Re = 148000$

b- Stresses: Figures 5, 6, and 7 show the Fields of the normal turbulent stresses and the shear stress.

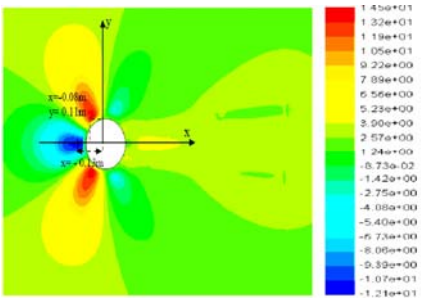

Fig. 5: Normal stress τ_{xx} / ρ

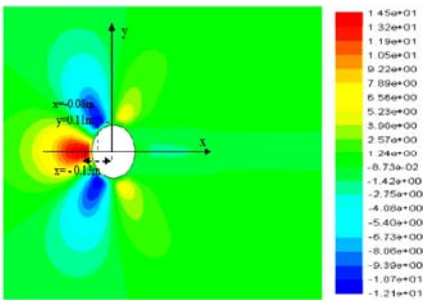

Fig. 6: Normal stress τ_{yy} / ρ

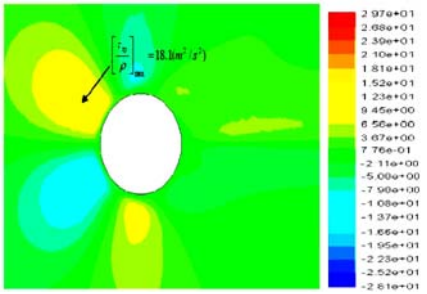

Fig. 7: Normal stress τ_{xy} / ρ

We find that all three components of stresses have significant values at upstream and downstream of the cylinder. This indicates that much of the turbulent stresses are actually created by the passage of Von Karman vortices that have a big importance relative to other energy turbulent stresses.

4.2 Evolution as a function of Reynolds number

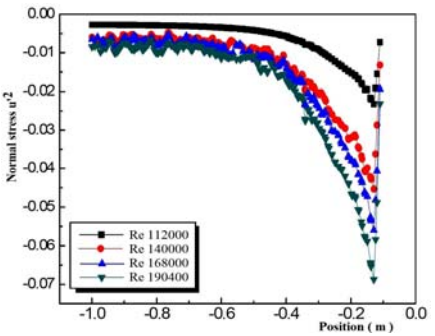

Fig. 8: Normal stress on the axis $y = 0\ (1 < x < 0)$ according to Reynolds

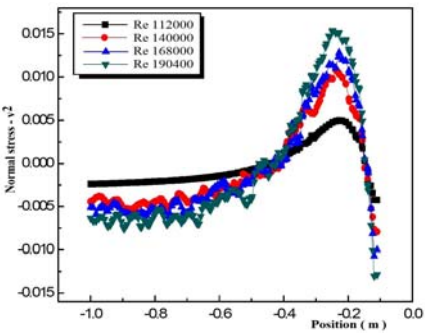

Fig. 9: Normal stress on the axis $y = 0\ (1 < x < 0)$ according to Reynolds

The profiles of turbulent normal stresses on the axis $y = 0$ are plotted in Figure 8, 9 for different Reynolds numbers.

The maxima of $\left|\frac{\tau_{xx}}{\rho}\right|$ and $\left|\frac{\tau_{yy}}{\rho}\right|$ is increasing by 50 % between $Re = 112000$ and $Re = 140000$.

This is explained by the predominance of gradients $\partial u / \partial x$ and $\partial v / \partial x$ when $112000 < Re < 140000$, knowing that $\frac{\tau_{xx}}{\rho} = \left(\nu_t 2\frac{\partial u}{\partial x} - \frac{2}{3}k \right)$ and $\frac{\tau_{yy}}{\rho} = \left(\nu_t 2\frac{\partial v}{\partial y} - \frac{2}{3}k \right)$.

5. VALIDATION OF RESULTS

The choice of a turbulence model depends on the types of fluid flow, of the order of accuracy, calculation equipments and available machine time.

In order to choose the most appropriate model for our application, we need to understand the capabilities and limitations of each model, [2].

The standard model $(k-\varepsilon)$ has been then applied to simulate the case of flow around a cylinder in a channel with flat bottom.

Calculation results were compared with those measures, [1]. The experimental data obtained allow making comparisons with the results of numerical simulation, not only for the velocities but also for the kinetic energy.

Before conducting the simulation of flow around a cylinder 2D, series of calculation tests are performed in the case of uniform flow and simple, to study the performance of this model, and to check some computational techniques adopted in this model.

All the simulation calculations are performed on a personal computer. The computation time is typically 2 hours for each test.

Comparisons between simulation results and those of the experiment for the profiles of velocity components and the kinetic energy k are detailed in this paper. All results are presented in the following sections: $\alpha_i =$ 0°, 45°, 90°, 135°, 157.5° and 180°.

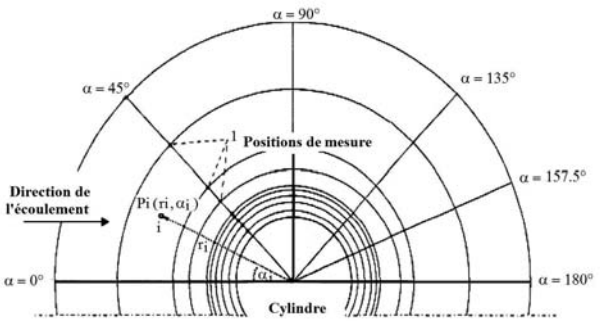

Fig. 10: Sections of measures taken

But we present here only the section 0°.

Section $\alpha = 0°$

a- Longitudinal velocity u

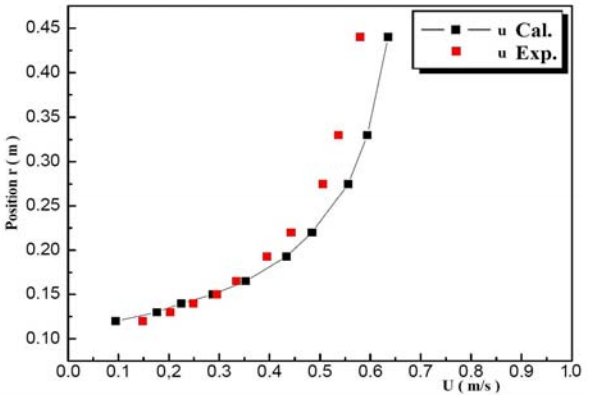

Fig. 11: Longitudinal velocity u at the section $\alpha = 0°$

Concerning the longitudinal velocity component U (Fig. 11), we notice that there is an agreement between the calculated and the experimental results. But with a mean squared error $\sigma_U = 0.117\ m/s$, which represents a relative error value $\sigma / \bar{u} = 0.174 = 17.4\%$.

Note also that the position of the maximum velocity (0.67 m/s) is far from the cylinder, but decreases when approaching the surface of the cylinder until the value

(0m/s) in the position $r = 0.11\,m$, which represents the breakpoint of the stream line according to section $\alpha = 0°$.

b- Transversal velocity v

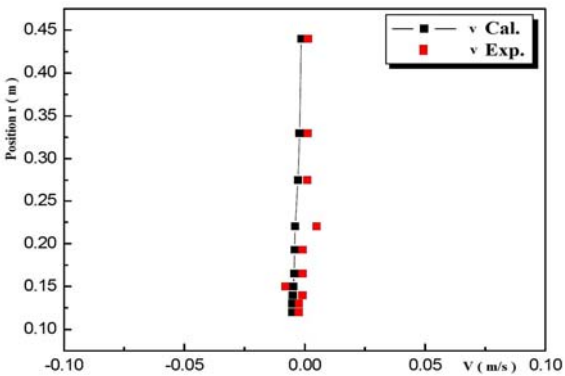

Fig. 12: Transversal velocity v at the section $\alpha = 0°$

The transverse velocity component v (Fig. 12), is practically zero in all points of the section $\alpha = 0°$. This can be explained by the symmetrical geometry of the system (centered cylinder between two parallel and similar plates), and a uniform flow at the entrance $u_0(0,y) = 0.67\ m/s$ and $v_0(0,y) = 0\ m/s$.

c- Kinetic energy k

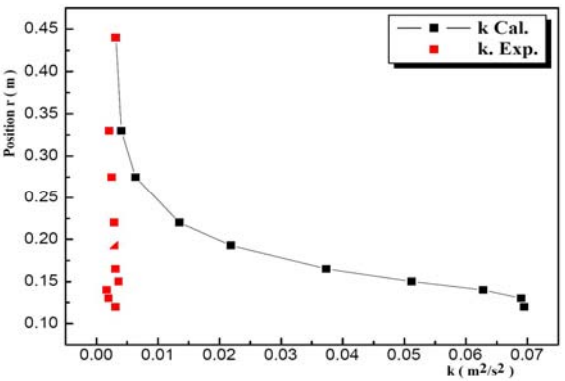

Fig. 13: Kinetic energy at the section $\alpha = 0°$

For the kinetic energy k (Fig. 13), there is a concordance between the calculated and the experimental results for positions that are far from the cylinder. While a divergence arises when one approaches it. The difference between the experimental and simulation becomes maximum $\Delta k = 0.065\,m^2/s^2$, when it reaches the position $r = 0.12\,m$, while the calculated values increase and the experimental values remain

almost constant. The mean square error in this section is $\sigma_k = 0.18\ m^2/s^2$, which represents a relative error value $\sigma / \overline{k} = 5.80$.

Hence, a bad result for the kinetic energy k is obtained with this model. There is no agreement between the experimental and simulation results in the adjacent zones to the wall (cylinder).

The same observations for the sections: $\alpha_i =$ 45°, 90°, 135°, 157.5° and 180°.

6. CONCLUSION

In this work, we obtained results of flow around the cylinder, using CFD code.

It is clear that the model ($k - \varepsilon$) standard can estimate the velocity components U and V with acceptable accuracy, but overestimates the kinetic energy turbulent especially in areas that are close to the wall (cylinder). It also underestimates the separation point, results are independent of the mesh, then the problem lies in the model chosen.

In fact, we must recognize that the modelling of turbulence is still until present a problem not fully resolved, and the existing models all have restrictions on use. Many researches are constantly undertaken to refine these models.

The flow around a circular cylinder has been investigated for large Reynolds numbers. The calculations were performed at Reynolds numbers of 112000, 148000, 168000 and 190400, with a focus on the Reynolds number 148000.

The analysis of the evolution of turbulent stresses quantities as a function of Reynolds number has shown two main consequences.

First, the recirculation region in the near wake is rising, when Reynolds goes on.

On the other hand, the turbulence absolute amounts increase sharply when the Reynolds number increases.

The perspectives of this work are numerous. From the side of the analysis of the flow, it is important to better analyze the strong three-dimensional effects. While this study showed that the mean flow was two-dimensional over a large part of the scope of the cylinder, the calculations on the plans (x , z) surly will show other characteristics of turbulent flow around the obstacles. It would be important to invest more in-depth of this effects.

From the standpoint of modelling, a review of various laws of closure can be achieved. In particular, non-alignment between the main directions of the turbulent stress tensor and tensor strain rate leads to a limitation of linear models based on the assumption of closure.

NOMENCLATURE

u , v , w : Instantaneous velocity components

u', v', w' : Fluctuations around the periodic motion

k : Kinetic-energy

ε : Dissipation of energy

$\overline{u'^2} = \frac{\tau_{xx}}{\rho}$: Normal stress

$\overline{v'^2} = \frac{\tau_{yy}}{\rho}$: Normal stress

$\overline{u'v'} = \frac{\tau_{xy}}{\rho}$: Shear stress

p : Pressure

REFERENCES

[1] B. Yulistiyanto, '*Flow Around a Cylinder Installed in a Fixed-Bed Open Channel*', Thèse de Doctorat, Ecole Polytechnique Fédérale de Lausanne, Switzerland, 1997.

[2] I. Istiarto, '*Flow Around a Cylinder on a Scoured Channel Bed*', Thèse de Doctorat, Ecole Polytechnique Fédérale de Lausanne, Switzerland, 2001.

[3] T.B. Gatski and T. Jongen, '*Nonlinear Eddy Viscosity and Algebraic Stress Models for Solving Complex Turbulent Flows*', Progress in Aerospace Sciences, Vol. 36, N°8, pp. 655 – 682, 2000.

[4] C. Norberg, '*LDV Measurements in the Near Wake of a Circular Cylinder*', Proceedings of the 1998. Conference on Bluff Body Wakes and Vortex-Induced Vibration, Washington, DC, USA, 1998.

[5] D. Choudhury, '*Introduction to the Renormalization Group Method and Turbulence Modeling*', Fluent Inc. Technical Memorandum TM-107, 1993.

[6] M. Van Dyke, '*An Album of Fluid Motion*', 172 p., Parabolic Press, Inc.; 12th Edition, 1982.